Anion solvation at the microscopic level: Photoelectron spectroscopy of the solvated anion clusters, $NO^-(Y)_n$, where Y=Ar, Kr, Xe, N_2O, H_2S, NH_3, H_2O, and $C_2H_4(OH)_2$

Jay H. Hendricks,[a] Helen L. de Clercq,[b] Carl B. Freidhoff,[c] Susan T. Arnold,[d] Joseph G. Eaton,[e] Chuck Fancher,[f] Svetlana A. Lyapustina,[g] Joseph T. Snodgrass,[h] and Kit H. Bowen[i]
Department of Chemistry, Johns Hopkins University, Baltimore, Maryland 21218

(Received 27 July 2001; accepted 15 January 2002)

The negative ion photoelectron spectra of the gas-phase, ion-neutral complexes; $NO^-(Ar)_{n=1-14}$, $NO^-(Kr)_1$, $NO^-(Xe)_{n=1-4}$, $NO^-(N_2O)_{n=3-5}$, $NO^-(H_2S)_1$, $NO^-(NH_3)_1$, and $NO^-(EG)_1$ [EG = ethylene glycol] are reported herein, building on our previous photoelectron studies of $NO^-(N_2O)_{1,2}$ and $NO^-(H_2O)_{1,2}$. Anion solvation energetic and structural implications are explored as a function of cluster size in several of these and as a result of varying the nature of the solvent in others. Analysis of these spectra yields adiabatic electron affinities, total stabilization (solvation) energies, and stepwise stabilization (solvation) energies for each of the species studied. An examination of $NO^-(Ar)_{n=1-14}$ energetics as a function of cluster size reveals that its first solvation shell closes at $n=12$, with an icosahedral structure there strongly implied. This result is analogous to that previously found in our study of $O^-(Ar)_n$. Inspection of stepwise stabilization energy size dependencies, however, suggests drastically different structures for $NO^-(Ar)_2$ and $O^-(Ar)_2$, the former being "Y" shaped, and the latter being linear. While stepwise stabilization energies usually provide good estimates of ion–single solvent dissociation energies, in the cases of $NO^-(Ar)_1$, $NO^-(Kr)_1$, and $NO^-(Xe)_1$, it is possible to determine more precise values. A plot of these anion–solvent dissociation energies shows them to vary linearly with rare gas atom polarizability, confirming the dominance of an ion-induced dipole interaction in these complexes. Extrapolation of this trend permits the estimation of $NO^- \cdots$ (rare gas atom) interaction energies for helium, neon, and radon, as well. The relative strengths of the molecular solvents, N_2O, H_2S, NH_3, H_2O, and EG are reflected in their stepwise stabilization energies and in the degree of broadening observed in their photoelectron spectra. © *2002 American Institute of Physics.*
[DOI: 10.1063/1.1457444]

I. INTRODUCTION

Anion solvation at the microscopic level is strongly influenced by the interaction between the negative ion, X^-, and the first few neutral solvents, Y, surrounding it. For this reason, the study of gas-phase anion–molecule complexes, $X^-(Y)_n$, containing relatively few solvent atoms or molecules, is of fundamental importance for understanding ion-solvation phenomena. For a given anion, X^-, the two parameters that can most easily be varied in such studies are the nature of the solvent, Y, and the number of solvents, *n*. Naturally, the variation of these can cause significant changes in the energetic, structural, and dynamic properties of the resulting cluster anion.

Over the past quarter century, both theory and experiment have sought to explore the effects of varying these parameters on anionic solvation at the microscopic level.[1] Calculations on anion–molecule complexes were among the earliest applications of theory to clusters.[2–19] Experiments have provided information about solvated cluster anions through thermochemical measurements,[20–30] photoelectron and photodetachment spectroscopies, ion–molecule reactivity studies,[31–35] ion transport measurements,[36,37] charge transfer work,[38,39] photodestruction studies,[40–49] photodissociation spectroscopy,[50–60] and ultrafast experiments.[61] Thermochemical measurements, especially those based on high-pressure mass spectrometry, were the earliest substantial sources of data on solvated cluster anions, and together with negative ion photoelectron spectroscopy, they thus far have supplied the majority of information about these species and the variation of their properties with the parameters, Y and *n*.

The first study to focus on the photodetachment of electrons from an anion–molecule complex was conducted on $OH^-(H_2O)_1$ in 1968 by Steiner, who obtained its photode-

[a]Also at: National Institute of Standards and Technology, Gaithersburg, MD 20899.
[b]Also at: Department of Chemistry, Howard University, Washington, DC 20059.
[c]Also at: Northrop-Grumman Corporation, Baltimore, MD 21203.
[d]Also at: Air Force Research Laboratory, Hanscom AFB, MA 01731.
[e]Also at: Department of Chemistry, North Dakota State University, Fargo, ND 58105.
[f]Also at: Stanford Research Systems, Sunnyvale, CA 94089.
[g]Also at: International Pharmaceutical Aerosol Consortium, Washington, DC 20005.
[h]Also at: Taylor Technology, Inc., Princeton, NJ 08540.
[i]Author to whom correspondence should be addressed. Electronic mail: kitbowen@jhunix.hcf.jhu.edu

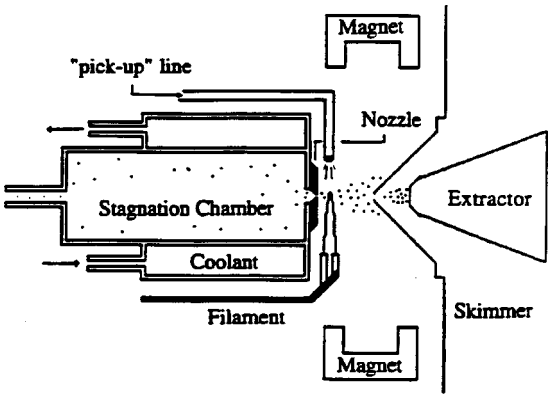

FIG. 1. A schematic diagram of the supersonic nozzle ion source used to generate $NO^-(Y)_n$ cluster anions in this work.

tachment threshold spectrum in a tunable wavelength experiment.[62] Negative ion photoelectron spectroscopy is a fixed wavelength approach to conducting photodetachment experiments. It utilizes electron energy analysis and yields line spectra rather than threshold spectra. The first study to apply this technique to a negative cluster ion was performed on $H^-(NH_3)_1$ in 1985 by our group.[63] Subsequently, negative ion photoelectron spectroscopy (both the continuous and the pulsed versions) became widely used in studying solvated cluster ions. We measured[63–72] the spectra of $NO^-(N_2O)_{n=1,2}$, $NH_2^-(NH_3)_{1-2}$, $H^-(NH_3)_{1-2}$, $NO^-(H_2O)_{n=1-2}$, $O_2^-(Ar)_1$, and $O^-(Ar)_{n=1-26,34}$. Lineberger[73] recorded the spectrum of $H^-(H_2O)_1$; Johnson[74–78] studied $O_2^-(H_2O)_1$, $O_2^-(N_2)_1$, $NO_2^-(N_2O)_1$, and $I^-(CH_3Cl)_1$; Cheshnovsky[79–81] investigated $I^-(H_2O)_{n=1-60}$, $Br^-(H_2O)_{n=1-16}$, $Cl^-(H_2O)_{n=1-7}$, and $Cl^-(NH_3)_1$; Neumark[82–84] examined $I^-(CO_2)_{n=1-13}$, $I^-(N_2O)_{n=1-12}$, and $Br^-(CO_2)_{n=1-11}$; and Nagata and Kondow[85] studied $[(CO_2)_nH_2O]^-$. In addition, Brauman[86–88] utilized tunable wavelength photodetachment to study $RO^-(HF)_1$ and $F^-(ROH)_1$ [R=organic group].

In this paper, we present the negative ion photoelectron spectra of several anion–neutral complexes in which the anion is NO^-. Nitric oxide plays a role in atmospheric photochemical cycles and in several important biological functions. Here, we examine the anion solvation energetics of $NO^-(Y)_n$, in some cases as a function of cluster size and in others as a result of changing the nature of the solvent. In the cases of $NO^-(Ar)_{n=1-14}$, $NO^-(Xe)_{n=1-4}$, and $NO^-(N_2O)_{n=3-5}$, we explore ion solvation as a function of cluster size (and thus in a stepwise manner), while in the cases of $NO^-(Kr)_1$, $NO^-(H_2S)_1$, $NO^-(NH_3)_1$, and $NO^-(EG)_1$ [EG=ethylene glycol], we investigate the effect of varying the nature (and thus the strengths) of the solvent on ion solvation. Combining the results of this study with those from our previous work on $NO^-(Y)_n$ species, we cumulatively have studied the effects of solvating NO^- with the simple atomic solvents; Ar, Kr, and Xe and with the more complex molecular solvents: N_2O, H_2S, NH_3, H_2O, and EG.

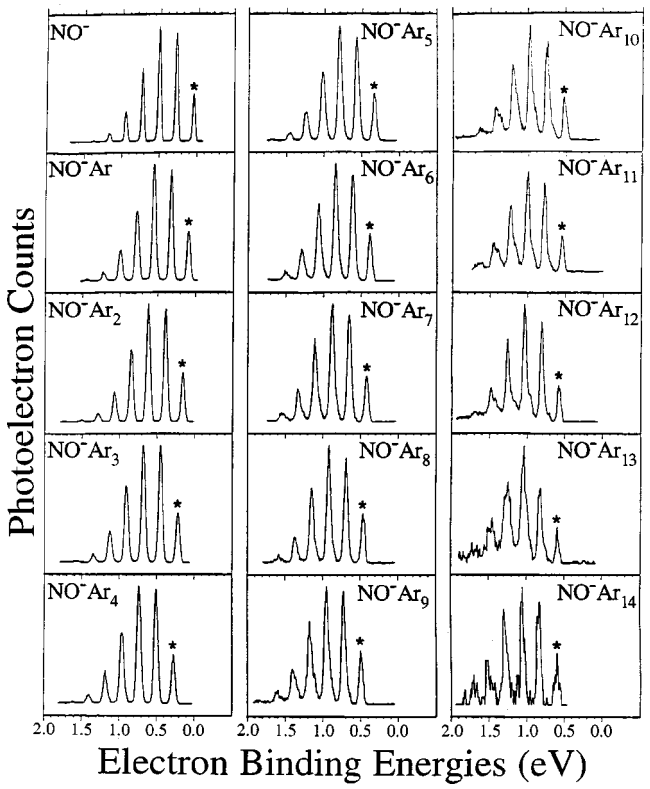

FIG. 2. The negative ion photoelectron spectra of $NO^-(Ar)_{n=0-14}$. The origin containing peak, i.e., the (0,0) transition, is labeled with an * on each spectrum.

II. EXPERIMENT

A. Apparatus

Negative ion photoelectron spectroscopy is conducted by crossing a mass-selected beam of negative ions with a fixed-frequency photo beam and energy analyzing the resultant photodetached electrons. Our negative ion photoelectron spectrometer has been described previously.[89] Anions generated in a supersonic expansion ion source are accelerated, collimated, and transported via a series of ion optical components, before being mass selected with an $\mathbf{E}\times\mathbf{B}$ Wien velocity filter. The mass-selected ion beam is then focused into a field-free, collision-free interaction region, where it is crossed with the intracavity photon beam of an argon ion laser operated at 488 nm (2.540 eV) and with a circulating power of 150–200 W. A small solid angle of the resulting photodetached electrons is accepted into the input optics of a magnetically shielded, hemispherical electron energy analyzer, where the electrons are energy analyzed and counted. Photoelectron spectra in this study were recorded with an instrumental resolution of 30 meV and were calibrated, before and after each new cluster anion spectrum, using the well-known photoelectron spectrum[90] of NO^-.

B. Cluster anion production

The cluster anions, $NO^-(Ar)_n$, were generated by expanding 8–10 atm of argon through a 12 μm nozzle into vacuum, while a small amount of N_2O was introduced into the plasma via a secondary effusive ''pick-up'' line located

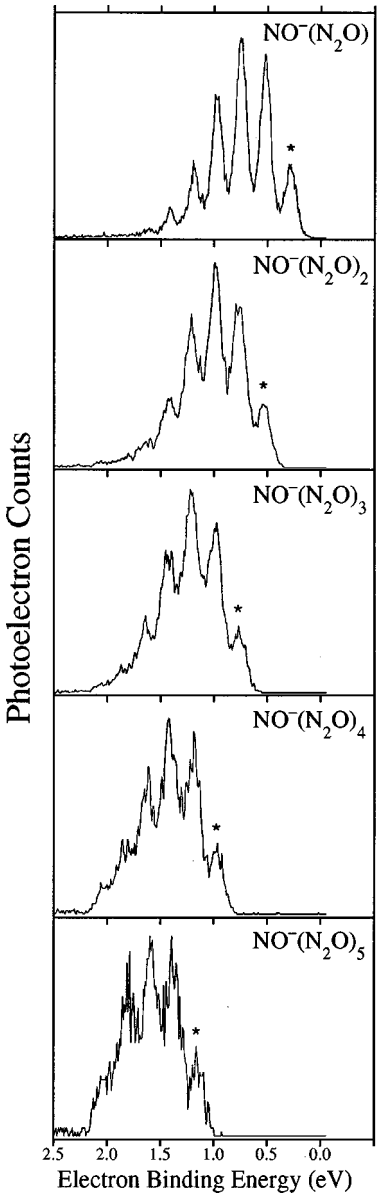

FIG. 3. The negative ion photoelectron spectra of $NO^-(N_2O)_{n=1-5}$.

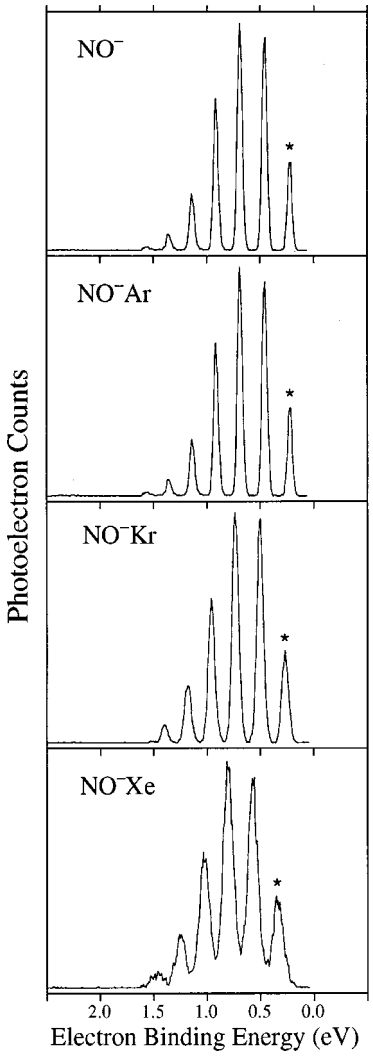

FIG. 4. The negative ion photoelectron spectra of NO^-, $NO^-(Ar)_1$, $NO^-(Kr)_1$, and $NO^-(Xe)_1$.

just above the nozzle. The source nozzle and cooling jacket temperatures were maintained at −70 °C by recirculating methanol through a dry ice/acetone temperature bath. This pick-up anion source is shown schematically in Fig. 1. A negatively biased filament (ThO_2/Ir) was used for ionization, forming NO^- anions from the N_2O pick-up gas, which then clustered with the cold argon expansion, forming $NO^-(Ar)_{n=1-14}$ cluster ion series. A predominantly axial magnetic field confined the plasma and enhanced cluster anion production. The cluster anions, $NO^-(Kr)_1$ and $NO^-(Xe)_{n=1-4}$ were generated under source conditions similar to those described above, except that 6 atm of a gas mixture containing 25% Kr/Ar or 10% Xe/Ar, respectively, was used behind the nozzle, and the source was maintained at 0 °C. Typical filament emission current and bias were 5–10 mA and −60 V, respectively.

For the production of $NO^-(N_2O)_{n=1-5}$, the same source shown in Fig. 1 was used. A supersonic expansion was created with 4 atm of N_2O behind a 17 μm nozzle maintained at −70 °C. No pick-up gas was used. Typical source conditions were 4 atm neat N_2O gas behind a 17 μm nozzle, and a source temperature of −70 °C. To generate $NO^-(H_2S)_1$, 2–3 atm of a 5% H_2S/Ar gas mixture was expanded through a 25 μm nozzle at a source temperature of −63 °C. Nitrous oxide was introduced through the pick-up line into the expanding supersonic jet. Typical filament emission current and bias were 8 mA and −100 V, respectively. Cluster anions of $NO^-(EG)_1$ were produced by coexpanding 2–3 atm of 0.3% EG/Ar gas mixture through a 25 μm nozzle at a source temperature between 60–90 °C. N_2O was introduced through the pick-up line. Typical filament emission current and bias were 25 mA and −90 V, respectively. $NO^-(NH_3)_1$ was similarly generated, using 2–3 atm of neat NH_3 gas behind the nozzle and introducing N_2O through the pick-up line.

III. RESULTS

The negative ion photoelectron spectra of $NO^-(Ar)_{n=0-14}$ are presented in Fig. 2, those for

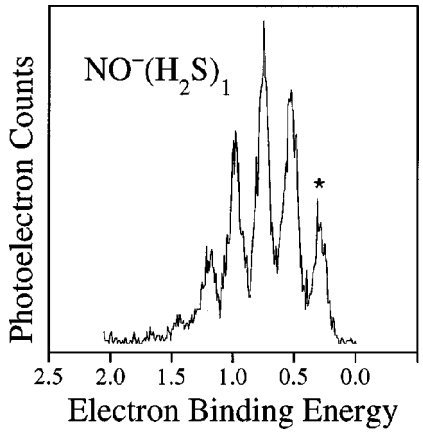

FIG. 5. The negative ion photoelectron spectrum of $NO^-(H_2S)_1$.

$NO^-(N_2O)_{n=1-5}$ are given in Fig. 3, those for NO^-, $NO^-(Ar)_1$, $NO^-(Kr)_1$, and $NO^-(Xe)_1$ are shown in Fig. 4, that of $NO^-(H_2S)_1$ is presented in Fig. 5, and that of $NO^-(EG)_1$ is presented in Fig. 6. The electron binding energy (EBE) of the origin transition's peak center in each spectrum is indicated with an asterisk (*), and this energetic information is tabulated in Tables I–V. This information is also included for the spectra of those ion–neutral complexes which were recorded, but not shown. From the origin transitions, adiabatic electron affinities (EA's), ion–solvent dissociation energies (D_0's), sequential or stepwise ion solvation energies (SE_{step}), and total ion solvation energies (SE_{total}) were determined as described in Sec. V below and also tabulated in Tables I–V.

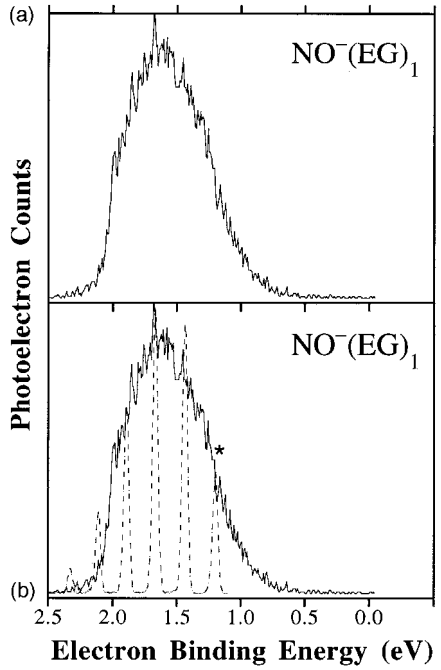

FIG. 6. (a) The negative ion photoelectron spectrum of $NO^-(EG)_1$ [EG = ethylene glycol]. (b) The $NO^-(EG)_1$ spectrum with the spectral profile of NO^- fit within it.

TABLE I. The values of EA, $SE_{step}(n)$, and SE_{tot} determined from the (0,0) origin peaks in the spectra of $NO^-(Ar)_{n=1-14}$ as described in the text. All energies in eV. (Typical error is ±3 meV for EBE's.)

n	(0,0) EBE[a]	EA[$NO(Ar)_n$]	$SE_{step}(n)$	SE_{tot}
0	0.044	0.026	⋯	⋯
1	0.102	0.084	0.058	0.058
2	0.168	0.150	0.066	0.124
3	0.226	0.208	0.058	0.182
4	0.283	0.265	0.057	0.239
5	0.338	0.320	0.055	0.294
6	0.390	0.372	0.052	0.346
7	0.428	0.410	0.038	0.384
8	0.466	0.448	0.038	0.422
9	0.498	0.480	0.032	0.454
10	0.529	0.511	0.031	0.485
11	0.553	0.535	0.024	0.509
12	0.584	0.566	0.031	0.540
13	0.598	0.580	0.014	0.554
14	0.607	0.589	0.009	0.563

[a]EBE = electron binding energy.

IV. CHARACTERIZATION OF $NO^-(SOLVENT)_n$ CLUSTERS

An important aspect of ion–neutral bonding concerns the distribution of excess negative charge over the negative cluster ion. One might imagine two extreme charge distribution categories; in one the excess charge is localized on a single component of the cluster ion, and in the other, the negative charge is dispersed over part or all of the cluster ion. The situation in which the excess charge is localized on a single component of the cluster ion is reminiscent of the usual notion of a solvated anion, where a central negative ion is surrounded by a sheath of neutral solvent molecules. There, the central negative ion may be thought of as remaining largely intact even though it is perturbed by its solvents. In this case, electrostatic interactions between the ion and solvent molecules presumably dominate the bonding. In other cases, however, charge dispersal effects may also make significant contributions to the bonding. These contributions may arise either in the sense of covalency in ion–neutral bonds or in the sense of excess electron delocalization via electron tunneling between energetically and structurally equivalent sites within the cluster ion. In favorable cases the photoelectron spectra of negative cluster ions can offer clues as to the nature of the excess charge distribution in these species.

TABLE II. The values of EA, $SE_{step}(n)$, and SE_{tot} determined from the (0,0) origin peaks in the spectra of $NO^-(Xe)_{n=1-4}$ as described in the text. All energies in eV. (Typical error is ±3 meV for EBEs.)

n	(0,0) EBE[a]	EA[$NO(Xe)_n$]	$SE_{step}(n)$	SE_{tot}
0	0.044	0.026	⋯	⋯
1	0.211	0.193	0.167	0.167
2	0.381	0.363	0.170	0.348
3	0.531	0.513	0.150	0.498
4	0.65	0.63	0.12	0.618

[a]EBE = electron binding energy.

TABLE III. The values of EA, $SE_{step}(n)$, and SE_{tot} determined from the (0,0) origin peaks in the spectra of $NO^-(N_2O)_{n=1-5}$ as described in the text. All energies in eV. (Typical error is ±3 meV for EBEs.)

n	(0,0) EBE[a]	EA[$NO(N_2O)_n$]	$SE_{step}(n)$	SE_{tot}
0	0.044	0.026	⋯	⋯
1	0.265	0.247	0.221	0.221
2	0.520	0.502	0.255	0.476
3	0.747	0.729	0.227	0.703
4	0.964	0.946	0.217	0.920
5	1.146	1.128	0.182	1.102

[a]EBE=electron binding energy.

The nomenclature, $NO^-(Y)_n$, implies that an intact NO^- ion interacts with, or is solvated by n neutral solvent molecules of Y, which is to say that the excess negative charge is essentially localized on the nitric oxide component of the cluster ion. In this solvated-ion (ion–neutral complex) bonding picture, the perturbed NO^- subion acts as a ''chromophore'' for photodetachment. This in turn leads to a photoelectron spectrum for the $NO^-(Y)_n$ cluster ion that closely resembles the photoelectron spectrum of free unperturbed NO^-, except for its features being shifted to higher electron binding energy (corresponding to increased stabilization) and perhaps, broadened.

The nitric oxide anion was the first molecular anion to be studied by negative ion photoelectron spectroscopy,[91] and as such, it has a very well-characterized photoelectron spectrum.[90] When an electron is attached to NO to form NO^-, it is accommodated in an antibonding orbital, and the nitrogen–oxygen bond length increases from 1.151 Å[92] in NO to 1.258 Å[91] in NO^-. (A NO^- bond length of 1.267 Å also appears in the literature.[93]) This structural difference between the anion and its corresponding neutral results in the photoelectron spectrum of NO^- being a vibrationally resolved envelope which exhibits (ν',ν'') transitions between the $\nu''=0$ vibrational level of NO^- and the $\nu'=0-6$ vibrational levels of NO. Transitions from higher ν'' levels of NO^- are not observed due to autodetachment. The transition, $NO\ (X\,^2\Pi,\nu'=0)\leftarrow NO^-(X\,^3\Sigma^-,\nu''=0)$, corresponds to the origin transition (0,0) and is labeled with an asterisk (*) in Figs. 2–6. When the center-of-mass electron kinetic energy corresponding to the center of this peak is subtracted from the photon energy (2.540 eV), one obtains a nominal electron affinity for NO of 0.044 eV. Consideration of rotational and spin–orbit effects leads to a correction of −0.018 eV to this value to yield the accepted value of 0.026 eV for the adiabatic electron affinity (EA)[90] of NO.

Our interpretation of the photoelectron spectra of $NO^-(Y)_n$ is that they can be viewed as the spectra of NO^- ions which have been perturbed to one extent or another by n solvent molecules, Y. We therefore assign the peak arising from the origin transition in the photoelectron spectrum of the NO^- subion to be the nominal adiabatic electron af-

TABLE IV. Spectral assignments, vibrational spacings, and relative peak intensities for the photoelectron spectra of NO^-, $NO^-(Ar)_1$, $NO^-(Kr)_1$, and $NO^-(Xe)_1$ are tabulated along with the electron binding energies (EBE) of their (0,0) origin peaks plus the extracted EA and anion–solvent dissociation energy, D_o, values. (Typical error is ±3 meV for EBEs.)

Assignment peak (ν',ν'')	Spacing between adjacent peaks (cm^{-1})	Normalized peak intensity	(0,0) EBE (eV)	EA[$NO(Ar)_1$] (eV)	D_o (eV)
NO^-					
(0,0)	⋯	0.121	0.044	0.026	⋯
(1,0)	1875	0.307			
(2,0)	1848	0.312			
(3,0)	1820	0.177			
(4,0)	1791	0.064			
(5,0)	1763	0.019			
$NO^-(Ar)$					
(0,0)	⋯	0.123	0.102	0.084	0.068
(1,0)	1895	0.283			
(2,0)	1873	0.298			
(3,0)	1820	0.193			
(4,0)	1796	0.078			
(5,0)	1749	0.025			
$NO^-(Kr)$					
(0,0)	⋯	0.118	0.143	0.125	0.111
(1,0)	1889	0.288			
(2,0)	1872	0.302			
(3,0)	1824	0.187			
(4,0)	1768	0.080			
(5,0)	1773	0.025			
$NO^-(Xe)$					
(0,0)	⋯	0.124	0.211	0.193	0.182
(1,0)	1887	0.283			
(2,0)	1862	0.303			
(3,0)	1792	0.186			
(4,0)	1778	0.077			
(5,0)	⋯	0.027			

finity of the respective $NO^-(Y)_n$ clusters. The same correction of -0.018 eV was then applied to these values. The resulting EA values for $NO(Y)_n$ clusters are listed in Tables I–V.

V. CLUSTER ION ENERGETICS

The energetic relationships between the generic solvated anion clusters, $X^-(Y)_n$, and their corresponding neutral clusters, $X(Y)_n$, are expressed through the identities

$$\mathrm{EA}[X(Y)_n] = \mathrm{EA}[X] + \sum_{m=0}^{n-1} D[X^-(Y)_m \cdots Y] - \sum_{m=0}^{n-1} D_{\mathrm{WB}}[X(Y)_m \cdots Y], \quad (1)$$

and

$$\mathrm{EA}[X(Y)_n] = \mathrm{EA}[X(Y)_{n-1}] + D[X^-(Y)_{n-1} \cdots Y] - D_{\mathrm{WB}}[X(Y)_{n-1} \cdots Y], \quad (2)$$

where $\mathrm{EA}[X(Y)_n]$ denotes the adiabatic electron affinity, $D[X^-(Y)_m \cdots Y]$ is the ion–neutral dissociation energy for the loss of a single solvent, Y, from a given cluster anion, and $D_{\mathrm{WB}}[X(Y)_m \cdots Y]$ is the analogous neutral cluster weak-bond dissociation energy for the loss of a single solvent, Y, from a given neutral cluster. Naturally, both of these dissociation energies are D_o's rather than D_e's. Since ion–solvent interaction energies generally exceed van der Waals bond strengths, it is evident from Eq. (1) that clustering can be expected to stabilize the excess electronic charge on a negative ion, i.e., the electron affinities of clusters should increase with cluster size. An example of this is seen in the photoelectron spectra of $NO^-(Y)_n$, where the subion is stabilized as the number of solvent atoms increases, shifting the spectra toward higher and higher electron binding energies. Eventually, however, as the mean number of solvent neighbors interacting with the anion becomes constant, this trend should reach a limit, and cluster electron affinities will become independent of cluster size. For these reasons, one expects EA values to increase relatively rapidly with cluster size for small n and then to approach a limiting value at some larger n. At still another level of refinement, one may anticipate the existence of structured EA versus n envelopes, due to unusually stable species such as those associated with filled solvation shells.

TABLE V. EAs and stepwise stabilization energies, $SE_{step}(1)$'s, determined from the (0,0) peaks in the spectra of the $NO^-(\text{molecular solvent})_1$ complexes reported here. All energies are in eV. (Typical error is ±20 meV for EBEs.)

Species	(0,0) EBE[a]	EA[NO(Solvent)]	SE_{step}
NO^-	0.044	0.026	⋯
$NO^-(N_2O)_1$	0.265	0.247	0.221
$NO^-(H_2S)_1$	0.286	0.268	0.242
$NO^-(NH_3)_1$	0.50	0.48	0.45
$NO^-(H_2O)_1$	0.77	0.75	0.72
$NO^-(EG)_1$	1.22	1.20	1.17

[a]EBE = electron binding energy.

From Eq. (2) it follows that the relationship between electron affinities of adjacent-sized $NO^-(Y)_n$ clusters can be expressed as

$$\mathrm{EA}[NO(Y)_n] - \mathrm{EA}[NO(Y)_{n-1}] = D_o[NO^-(Y)_{n-1} \cdots Y] - D_{\mathrm{WB}}[NO(Y)_{n-1} \cdots Y]. \quad (3)$$

The change in a cluster's EA upon the addition of a single solvent is the stepwise or sequential stabilization (solvation) energy, SE_{step}

$$SE_{step}(n) = \mathrm{EA}[NO(Y)_n] - \mathrm{EA}[NO(Y)_{n-1}]. \quad (4)$$

Substitution of Eq. (4) into Eq. (3) leads to an expression for a given cluster anion single solvent dissociation energy in terms of $SE_{step}(n)$ and D_{WB}

$$D_o[NO^-(Y)_{n-1} \cdots Y] = SE_{step}(n) + D_{\mathrm{WB}}[NO(Y)_{n-1} \cdots Y]. \quad (5)$$

The neutral–neutral interaction energy (D_{WB}) in Eq. (5) is typically substantially smaller than the ion–solvent interaction energy (D_o), and so in cases where D_{WB} is not known, its relatively minor contribution may be neglected, resulting in the relatively good approximation that the anion single solvent dissociation energy is essentially equal to the sequential solvation energy

$$D_o[NO^-(Y)_{n-1}Y] \approx SE_{step}(n). \quad (6)$$

The total stabilization (solvation) energy $SE_{tot}(n)$ is the difference between the EA of a given $NO(Y)_n$ cluster and the EA of NO (which is also equal to the sum of all the individual sequential stabilization energies for a given cluster ion of size, n)

$$SE_{tot}(n) = \mathrm{EA}[NO(Ar)_n] - \mathrm{EA}[NO],$$

$$SE_{tot}(n) = \sum_{m=1}^{n} SE_{step}(m). \quad (7)$$

Again, given that weak bond dissociation energies are not always known, substitution of Eq. (6) into Eq. (7) shows that $SE_{tot}(n)$ is an approximation to the total ion–solvent dissociation energy of a given $NO^-(Y)_n$ cluster

$$SE_{tot}(n) \approx \sum_{m=1}^{n} D[NO^-(Y)_{m-1} \cdots Y]. \quad (8)$$

In the following sections, the results presented in this paper are interpreted in terms of Eqs. (1)–(8).

VI. INTERPRETATION AND DISCUSSION

A. $NO^-(Ar)_{n=1-14}$, $NO^-(Xe)_{n=1-4}$, and $NO^-(N_2O)_{n=1-5}$

Our previous photoelectron study of $O^-(Ar)_n$ explored the solvation of a monatomic anion by simple monatomic solvents, which themselves interact with one another only weakly.[69] In the present study of $NO^-(Ar)_n$, additional elements of complexity have been added by making the ion a heteronuclear diatomic molecular anion. As in the case of $O^-(Ar)_n$, in this study there are three main types of information to be interpreted: total stabilization energy versus cluster size data (SE_{tot} versus n), the appearance of any

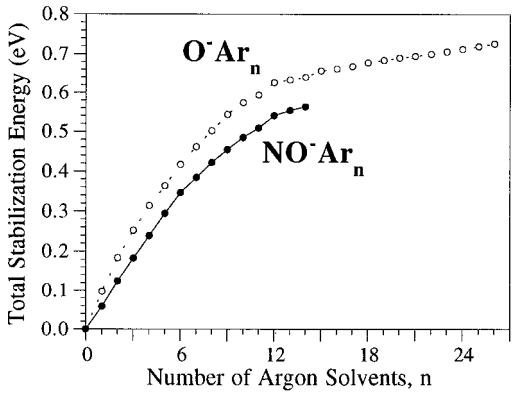

FIG. 7. The total stabilization (solvation) energy (SE_{tot}) of $NO^-(Ar)_n$ as a function of the number of argon atoms per cluster anion. The SE_{tot} values for $O^-(Ar)_n$ are also presented in this figure for comparison.

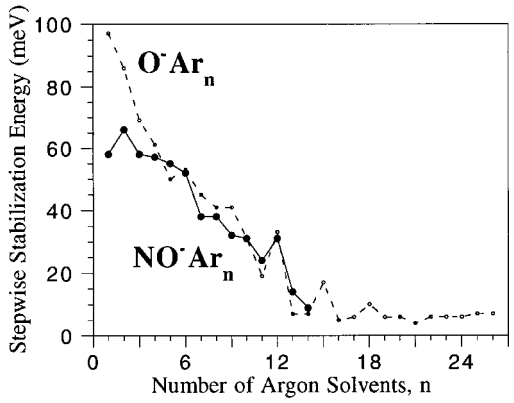

FIG. 8. The stepwise stabilization energies (SE_{step}) of $NO^-(Ar)_n$ as a function of cluster size. The SE_{step} values for $O^-(Ar)_n$ are also presented in this figure for comparison. (Typical errors for these data were ± 5 meV or less.)

magic numbers in the mass spectrum, and stepwise stabilization energy versus cluster size data (SE_{step} versus n). The photoelectron spectra of $NO^-(Ar)_{n=1-14}$ are presented in Fig. 2, and the energetic information extracted from them is given in Table I.

In Fig. 7, the SE_{tot} values of both $NO^-(Ar)_n$ and $O^-(Ar)_n$ are plotted as a function of cluster size (number of argon atoms per cluster ion). For both systems, the size dependencies of SE_{tot} show smoothly increasing trends through $n=12$, at which point a decrease in the values of their slopes occurs. This is obvious at a glance for $O^-(Ar)_n$, where the data extend out to $n=26$, and upon closer inspection of the data, it is also seen to be the case for $NO^-(Ar)_n$. Thus, for $n>12$, the average stabilization energy per argon atom decreases for both systems, implying that additional argon atoms beyond $n=12$ are being shielded from the subion. This is interpreted for $NO^-(Ar)_n$, as it was previously for $O^-(Ar)_n$, as evidence that the first solvation shell around the subion closes with the addition of the 12th argon atom, and it suggests, in analogy with $O^-(Ar)_n$, that the structure of this closed solvation shell is an icosahedral cage with the ion inside.

Although the size dependencies of SE_{tot} for $NO^-(Ar)_n$ and $O^-(Ar)_n$ are indeed similar to each other in most respects, $SE_{tot}(n)$ values for $NO^-(Ar)_n$ are consistently smaller than $SE_{tot}(n)$ values for $O^-(Ar)_n$ of the same size, n. This is presumably due to NO^- having a more diffuse excess electron distribution than O^-. Said differently, the trends in Fig. 7 suggest (if they can be assumed to continue with size) that NO^- will have a smaller total stabilization energy in bulk argon than will O^-. Bulk solvation energies can be estimated using the Born equation, and they are inversely proportional to R_i, the radius of the ion. Thus, for a given solvent, the larger of the two ions, i.e., NO^-, is expected (consistent with the argument above) to have the smaller total stabilization energy in bulk, essentially because its excess charge occupies the greater volume, i.e., its excess electron distribution is more diffuse.

Returning to the issue of the first shell closing in $NO^-(Ar)_n$, evidence that it occurs at $n=12$ is also provided by mass spectral data. We observed a single magic number, at $n=12$, in the mass spectrum of $NO^-(Ar)_n$. The closing of the first solvation shell in $NO^-(Ar)_n$ at $n=12$ and our interpretation of its structure as being icosahedral are also consistent with mass spectral studies of the cationic clusters, $NO^+(Ar)_n$, by Feigerle and Miller.[94] Their cation mass spectrum contained a magic number at $n=12$ which was attributed to the formation of an icosahedral structure with NO^+ inside a cage of argon solvents.

The size dependence of stepwise stabilization energies also provides strong evidence for a solvation shell closing at $n=12$ both in $NO^-(Ar)_n$ and in previously studied $O^-(Ar)_n$, and both of these plots are shown in Fig. 8. The stepwise stabilization energy, SE_{step}, is the change in the electron affinity of a given cluster upon the addition of a single solvent [see Eq. (4)]. Also, the dissociation energy for a given cluster anion losing a single solvent is given by Eq. (5), and it is approximately equal to the stepwise stabilization energy. Thus, $SE_{step}(n)$ represents the additional stabilization energy acquired by a cluster anion of size, n, by the addition of the nth solvent atom or molecule. To first order, one expects the size dependence of SE_{step} to decrease monotonically with n, since the interaction between an ion and its first few solvents is expected to be the strongest, and the stabilizing effect of each additional solvent tends to diminish as the cluster ion grows. Deviations from this expectation are the result of the presence of unusually stable structures. Generally speaking, both $NO^-(Ar)_n$ and $O^-(Ar)_n$ follow the expected trend, and there is a remarkable quantitative similarity between most of the data for these two systems. However, in both series, local maxima are seen in these plots, indicating enhanced stability for specific sizes of cluster anions. The largest single local maximum in the SE_{step} plot for $O^-(Ar)_n$ occurs at $n=12$, followed by an abrupt drop in SE_{step} for $n=13$ and $n=14$. Consistent with our interpretation based on $SE_{tot}(n)$ and mass spectral data, this is taken to be additional evidence for an unusually stable structure at $n=12$, specifically the closing of the first solvation shell around O^- by an icosahedral cage of argon atoms. The sharp drops in SE_{step} values at $n=13$ and $n=14$ are consistent with the 13th and 14th argons sensing an O^- subion that is substantially shielded by the cage, i.e., the sheath of 12 argons comprising its first closed solvation shell. The situation for

$NO^-(Ar)_n$ at $n=12$ is completely analogous to that of $O^-(Ar)_n$ at the same size. The SE_{step} versus n plot for $NO^-(Ar)_n$ also shows a local maxima at $n=12$, with abrupt drops in SE_{step} values at $n=13$ and 14. As in the case of $O^-(Ar)_{12}$, our interpretation of $NO^-(Ar)_{12}$'s structure is that the NO^- anion sits inside an icosahedral cage of 12 argon atoms. Interestingly, the value of SE_{step} at $n=12$ is nearly identical for both systems. This is essentially the energy required to remove one argon atom from the icosahedral cage, i.e., to disrupt it. The fact that this energy should be indifferent to whether O^- or NO^- is inside (given that both can fit there) is consistent with the structure at $n=12$ being an unusually stable cage.

One might expect that differences between the solvation of a spherical ion, such as O^-, and a rod-like ion, such as NO^-, by a common solvent would be most pronounced with relatively small numbers of solvents, and that is what we see in Fig. 8. In addition to $NO^-(Ar)_n$ displaying smaller SE_{step} values than does $O^-(Ar)_n$ for the first few numbers of solvents, a second local maximum is also seen in the stepwise stabilization energy plot for $NO^-(Ar)_n$, and it occurs at $n=2$. Such a local maximum does not occur among the first few solvents in the SE_{step} plot for $O^-(Ar)_n$, and its occurrence at $n=2$ in $NO^-(Ar)_n$ is, at first sight, unexpected. Nevertheless, it was observed repeatedly in data set after data set, and we believe it to be real. Calculations by Chalasinski[95] found the global minimum structure of $NO^-(Ar)_1$ to be a collinear structure, either $[Ar\cdots(O-N)^-]$ or $[Ar\cdots(N-O)^-]$, with the former structure being slightly lower in energy. While these calculations did not specifically explore the potential surface of $(NO)^-Ar_2$, one might expect, based on examining the $(NO)^-Ar_1$ surface, that a second argon would attach itself to the other end (the nitrogen end) of NO^-. If so, this would not result in the SE_{step} for $n=2$ increasing in value over that of $n=1$, as is actually observed. Based on the experimental evidence, it seems more likely that the second argon atom is adding to the same end of NO^- as did the first, forming a Y-shaped structure for $(NO)^-Ar_2$. In this case, the second argon would be stabilized not only by the $NO^-\cdots Ar$ interaction energy ($\sim$58 meV), but also by the $Ar\cdots Ar$ interaction energy, which is $\sim$12 meV.[96,97] Consistent with this, the measured increase in SE_{step} for $n=2$ over that for $n=1$ is 8 meV.

While the present study is certainly not a structural determination, it is interesting to speculate, based on our data and available theoretical guidance, about the structures of the $NO^-(Ar)_n$ cluster anions having several more argon solvents. Using Monte Carlo methods, Amar[98] has calculated the minimum energy structures for $Br_2^-(Ar)_{n=2-13}$, thereby examining the structures of a different diatomic anion solvated by argon atoms. Some of what he found for $Br_2^-(Ar)_n$ may be analogous to $NO^-(Ar)_n$, while some of it is not. For example, he found that $Br_2^-(Ar)_{11}$ forms a particularly stable structure of icosahedral geometry, with one bromine atom residing inside the icosahedral argon cage and with the other bromine atom forming part of the wall of the cage. This is different from what we observe for $NO^-(Ar)_n$. We see a prominent SE_{step} feature at 12 argons, but not at 11 argons, implying that the entire NO^- subion is inside the cavity, and that it does not form part of the skin of the cage. Amar also found that the first five rare-gas solvent atoms add around the waist of the homonuclear diatomic molecular anion, Br_2^-. Figure 8 shows that $NO^-(Ar)_n$'s SE_{step} values, while decreasing gradually from $n=3-6$, are actually fairly constant there, falling precipitously only by $n=7$. (We see nothing special at $n=5$.) Could this "shelf" between $n=3-6$ be the result of four argon atoms (the 3rd through the 6th) adding themselves around the waist of the NO^- subion? If one assumes that all of the foregoing is valid and then combines it to make an educated guess, $NO^-(Ar)_6$ could be envisioned with two of its argon atoms bound to the oxygen end of NO^- in a Y configuration and with the other four argon atoms distributed around the waist of the NO^- subion's molecular axis. This would look somewhat like a "Pac-man" structure, with the ion largely covered, but not completely enveloped in argon atoms.

The photoelectron spectra of $NO^-(Xe)_{n=1-4}$ all exhibit the now familiar spectral fingerprint of the NO^- subion, just shifted to higher electron binding energies with increasing cluster size and broadened. Energetic information, extracted from these spectra, is presented in Table II. We did not follow this series up far enough in cluster size to see the closing of the first solvation shell, but the qualitative trend in the size dependence of SE_{step} is interesting. It shows a small local maxima at $n=2$ (see Table II), just as $NO^-(Ar)_n$ did. The magnitude of the energy difference between SE_{step} at $n=1$ and SE_{step} at $n=2$ is less than expected, based on the foregoing discussion, but this may be misleading, since the data quality for this system was somewhat lower than that for $NO^-(Ar)_n$. The significant point here is that SE_{step} does not decrease smoothly from $n=1$ to $n=2$, as it does in substantial increments from $n=2$ to $n=3$ and from $n=3$ to $n=4$. In fact, SE_{step} increases slightly from $n=1$ to $n=2$.

In a previous study, we reported[64] on the photoelectron spectra of $NO^-(N_2O)_{n=1,2}$. Here, we add $NO^-(N_2O)_{n=3-5}$ to this series, providing cumulative data on $NO^-(N_2O)_{n=1-5}$. The photoelectron spectra of $NO^-(N_2O)_{n=1-5}$ are presented in Fig. 3, and energetic information extracted from them is given in Table III. Here, as in the case of $NO^-(Xe)_n$, we have not followed the $NO^-(N_2O)_n$ series up in size far enough to see the closing of its first solvation shell, but the trend in the size dependence of SE_{step} is again interesting at small sizes. Inspection of the SE_{step} versus n data for $NO^-(N_2O)_{n=1-5}$ in Table III reveals that, in this system as well, there is a pronounced local maxima at $n=2$. Local maxima in SE_{step} versus n plots have their origin in attractive, neutral–neutral interactions. The increase in SE_{step} in going from $n=1$ to $n=2$ is 34 meV, and while the interaction energy between two neutral nitrous oxide molecules is apparently not known, $\sim$30–40 meV is probably a reasonable estimate of its actual value. This supports the hypothesis that the first two solvents bind relatively close to each other at one end of the NO^- subion, in order to get stabilization from both $NO^-\cdots$solvent and solvent–solvent interactions. If, as appears to be the case, the occurrence of local SE_{step} maxima at small cluster sizes is due to some specific property of NO^- and how it interacts with solvents, then it would be interesting to see whether SE_{step}

size dependencies for $O^-(Y)_n$ species show the same effect. In fact, we have already seen that $O^-(Ar)_n$ exhibits no such local maxima at $n=2$ in its SE_{step} size dependence, nor for that matter does it show any local maxima below $n=6$. Also, while we do not have data for $O^-(N_2O)_n$, it is noteworthy that neither our $O^-(Kr)_{n=1-5}$ nor our $O^-(Xe)_{n=1-3}$ photoelectron data show any local maxima in their SE_{step} size dependencies.[99] So, why should $NO^-(Y)_n$, but not $O^-(Y)_n$, exhibit local SE_{step} maxima at $n=2$? After all, it might seem that if the second solvent in $NO^-(Y)_2$ gets its stabilization from the combination of both $NO^-\cdots Y$ and $Y\cdots Y$ interactions, then the second solvent in $O^-(Y)_2$ should do the same, giving rise to a local maxima at $n=2$ in the SE_{step} size dependence of $O^-(Y)_n$. While the anisotropy of the $NO^-\cdots$solvent potential is presumably at the root of the reason for why the first two solvents attach themselves to the same end of NO^- in $NO^-(Y)_2$, we postulate the following explanation for why the first two solvents to attach onto O^- apparently do not interact closely with one another. The electronic configuration of O^- is $1s^22s^22p^5$, and rare-gas atoms often act as weak bases in the bonding of weakly bound complexes. Since linear N_2O is a very poor acid, it probably acts as a weak base as well. Thus, the first two solvents should preferentially interact with the one half-filled p orbital of O^-. This would result in a linear structure for $O^-(Y)_2$, e.g., $Ar\cdots O^-\cdots Ar$, with the first two solvents well separated from one another at the opposite lobes of the operative p orbital. Recently, Fajardo has performed calculations that support our contention that $O^-(Ar)_2$ is linear with the O^- ion in the middle.[100] Of course, as more solvents are added, the stabilization from solvent$\cdots$solvent interactions will begin to come into play, but by then, it will act principally to moderate the descending slope of the SE_{step} versus n plot. Exceptions will be those structures which have unusual stability by virtue of their especially attractive solvent$\cdots$solvent interactions.

Furthermore, an interesting development has occurred since our original paper on $NO^-(N_2O)_{n=1,2}$. Hiraoka, using high-pressure mass spectrometric techniques, has reported thermochemical evidence for covalent bond formation in $NO^-(N_2O)_1$, i.e., $N_3O_2^-$ and higher clusters.[101] His and our experiments are mutually complementary, but both have their blind spots on this issue. It is rather challenging in his experimental environment to make and to maintain an anion as delicate as NO^- (NO has a low EA). In our experiment, we do not yet have the ultraviolet photons available that would likely be necessary to detect the presence of anions such as $N_3O_2^-$ by photodetachment (N_3O_2 probably has an EA by >2.5 eV). Nevertheless, it is evident from the NO^- fingerprint seen in our photoelectron studies that $NO^-(N_2O)_{n=1,2}$ as well as $NO^-(N_2O)_{n=3-5}$ all exist, at least initially, as anion–molecule complexes with intact N O^-subions. Hiraoka's experiment operates on an inherently longer time scale than ours (seconds versus milliseconds), and interestingly, his results seem to imply that, given enough time and collisions, at least some of the $NO^-(N_2O)_n$ ion–molecule complexes that we observe will internally react to form covalent anions and clustered covalent anions of the form $N_3O_2^-(N_2O)_m$. Our present studies of $NO^-(N_2O)_{n=3-5}$ take on added significance in this light, given that they provide significantly more reactants ''onboard'' the cluster ion and thus more opportunity for internal ion–molecule reactions than did our earlier work with smaller cluster ions. Still, we see strong spectroscopic evidence for the presence of intact NO^- subions in the larger as well as the smaller of these species. Nevertheless, the anionic products of internal ion–molecule reactions involving cluster ions of nitrogen oxides may well be occurring side by side with anion–molecule complexes, as implied by the combination of Hiraoka's and our work together. Another example of the formation of covalent anions in clusters may be found in the Rydberg electron transfer studies of nitric oxide clusters by Carman,[38] in which he proposed the formation of a $(NO)_3^-$ core solvated by nitric oxide dimers, i.e., $(NO)_3^-[(NO)_2]_x$.

B. $NO^-(Ar)_1$, $NO^-(Kr)_1$, $NO^-(Xe)_1$

Thus far in this paper, we have examined the gas-phase solvation of nitric oxide anions as a function of cluster size. Now, we consider the effect on their solvation caused by changing the nature of the solvent in single solvent complexes. In this particular section, we present a comparative study of the relatively simple complexes, $NO^-(Ar)_1$, $NO^-(Kr)_1$, $NO^-(Xe)_1$. Inspection of their photoelectron spectra in Fig. 4 reveals the well-known spectral signature of NO^- in every case. While this fingerprint pattern shifts to higher EBEs and broadens in going from $NO^-(Ar)_1$ to $NO^-(Kr)_1$ to $NO^-(Xe)_1$, Table IV shows that neither their vibrational spacings nor their relative peak intensities have been altered significantly upon solvation with single rare-gas solvents. If the interaction between NO^- and any of these rare-gas solvents had been strong enough to change the NO^- bond length, this would have revealed itself, as it did in our previous study[64] of $NO^-(N_2O)_1$, through a measurable change in the Franck–Condon profile (the relative peak intensities) of the NO^- subion pattern. The fact that it did not supports the contention that these are simple systems in which the rare-gas atom only weakly perturbs the NO^- subion. Nevertheless, the excess electron on a nitric oxide anion is stabilized to some extent by its interaction with a rare-gas solvent, and the degree of its stabilization is reflected directly in its electron affinity, EA, and indirectly through its ion–single solvent dissociation energy, D_o. Equation (5) shows that D_o is the sum of SE_{step}, which we measure, and D_{WB}, which is usually relatively small, but not necessarily known. In the case of these systems, however, the neutral weak-bond dissociation energies, D_{WB}, are known, and they are $\sim$10, $\sim$12, and $\sim$15 meV for $NO(Ar)_1$, $NO(Kr)_1$, and $NO(Xe)_1$, respectively.[102–107] The availability of these numbers allows us to report D_o values by adding the corresponding values of SE_{step} and D_{WB}. They are: $D_o[NO^-\cdots Ar]=68\pm14$ meV, $D_o[NO^-\cdots Kr]=111\pm18$ meV, and $D_o[NO^-\cdots Xe]=182\pm23$ meV. The cited errors are the result of combining the reported error in D_{WB} values and our assessment of the error in measured SE_{step} values.

Inspection of Table IV sows that both EA and D_o for

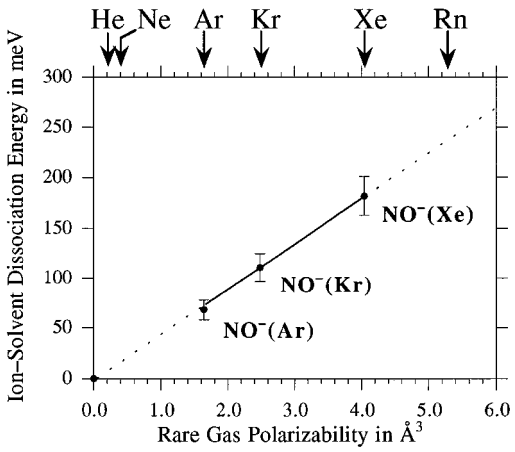

FIG. 9. A plot of the ion–solvent dissociation energies of $NO^-(Ar)_1$, $NO^-(Kr)_1$, and $NO^-(Xe)_1$ vs the polarizabilities of their corresponding rare-gas solvents. (The polarizability of each rare-gas atom is indicated by arrows at the top of the figure.) A linear relationship is evident, and its extrapolation is shown as a dotted line.

these ion–neutral complexes increase with increasing rare-gas atom polarizabilities, and Fig. 9 shows that the relationship between D_o and rare-gas atom polarizability, α, is linear. The D_o values reported here are, of course, also anion–solvent interaction energies, and the linearity of Fig. 9 implies that the ion-induced dipole interaction is the main interaction between a NO^- subion and a rare-gas atom, as expected. A linear least-squares fit of the three D_o versus α data points plus the origin as a fourth point results in a good, straight line having a correlation coefficient of 0.999. Extrapolation of this line (see Fig. 9) leads to estimates of ion–neutral dissociation energies for the complexes, $NO^-(He)_1$, $NO^-(Ne)_1$, and $NO^-(Rn)_1$. Using polarizability values of 0.205 Å^3, 0.396 Å^3, and 5.3 Å^3 for He, Ne, and Rn, respectively,[108–110] the resultant ion–neutral dissociation energies are $D_o[NO^-\cdots He]=7$ meV, $D_o[NO^-\cdots Ne]=16$ meV, and $D_o[NO^-\cdots Rn]=238$ meV. Interestingly, Chalasinski[95] has calculated $D_e[NO^-\cdots He]$ to be 8.7 meV.

The nitric oxide anion–radon interaction energy and the method of its determination are also noteworthy. Radon has two prominent physical properties: it is ''sticky'' (it has a large polarizibility), and it is radioactive. Because of the former, it may be possible to take advantage of its very substantial ion–neutral radon interaction energy to collect and concentrate the radon, either for analytical or for scrubbing purposes. Since the ion–neutral radon interaction energy is about an order of magnitude greater than the comparable neutral–neutral radon interaction energy (using $NO^-\cdots Rn$ and an extrapolation for $NO\cdots Rn$ as prototypes), the collection of radon by ion precipitation or high surface area ion adsorption might potentially be more effective than presently used neutral adsorption techniques. (Conversely, the adsorption of radon on charged biological surfaces and on charged airborne particulates might be more dangerous to health than its weaker adsorption on uncharged biological surfaces and neutral dust/smoke particles.) Because radon is radioactive and has a short half-life, it is also unlikely that one would elect to measure ion–neutral radon interaction energies directly. Given the linear relationship between ion–rare-gas atom interaction energies and rare-gas atom polarizabilities, this extrapolation approach is probably a general method for indirectly obtaining ion–neutral radon interaction energies for arbitrary ions. Such numbers might be useful in designing ion-based radon collection media.

While still on the subject of ion-induced dipole interactions, it is interesting to consider how much they contribute to total anion–molecule interaction energies. For example, the (total) ion–neutral dissociation energies of $NO^-(N_2O)_1$ and $NO^-(H_2O)_1$ were previously determined in our lab to be 258 meV[64] and 720 meV,[68] respectively, using the approximation in Eq. (6). Based on polarizabilities alone, extrapolations from the linear fit in Fig. 9 predict D_o's of only ~120 and ~60 meV for $NO^-(N_2O)_1$ and $NO^-(H_2O)_1$, respectively. Thus, for $NO^-(N_2O)_1$, ~45% of its total ion–neutral dissociation energy is due to ion-induced dipole interactions, with most of the remainder presumably due to ion–permanent dipole interactions. For $NO^-(H_2O)_1$, on the other hand, where the solvent is both polar and capable of strong hydrogen bonding, only ~8% of its total ion–neutral interaction energy is due to ion-induced dipole interactions.

In the cases of $NO^-(Ar)_1$ and its corresponding neutral, $NO(Ar)_1$, there is enough additional information available to make unique refinements to our analysis. As noted earlier, Chalasinski has conducted theoretical calculations on $NO^-(Ar)_1$, finding its global minimum to correspond to a collinear structure.[95] Furthermore, scattering experiments by Thuis[104] and by Casavecchia,[105] and theoretical calculations by Alexander[107] have provided potential energy curves that show the global minimum of neutral $NO(Ar)_1$ to correspond to a ''T''-shaped geometry. Since photodetachment is a vertical process, transitions from the ground state of the anion will access the neutral's potential surface at the geometry of the anion. By locating $NO^-(Ar)_1$'s calculated ground-state geometry on $NO(Ar)_1$'s potential surface, one finds that the photodetachment of electrons from $NO^-(Ar)_1$ accesses the neutral's potential surface ~4 meV above the energy of $NO(Ar)_1$'s T-shaped, global minimum configuration. In this light, our reported EA for $NO(Ar)_1$ of 84 ± 5 meV is slightly

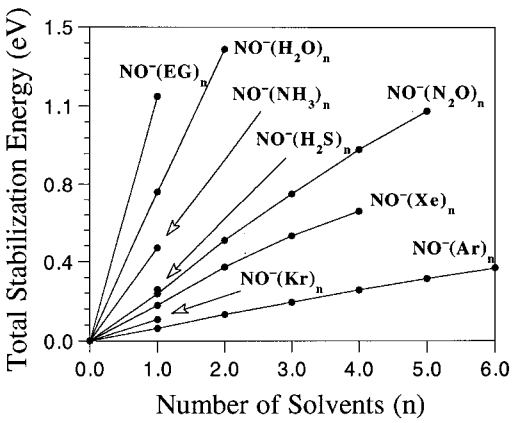

FIG. 10. Summary of SE_{tot} vs n results for $NO^-(Ar)_{n=1-6}$, $NO^-(Kr)_1$, $NO^-(Xe)_{1-4}$, $NO^-(N_2O)_{n=1-5}$, $NO^-(H_2S)_1$, $NO^-(NH_3)_1$, $NO^-(H_2O)_{n=1-2}$, and $NO^-(EG)_1$. (Results for $NO^-(Ar)_{7-14}$ are not shown on this graph due to lack of space.)

too large, and it should be refined by -4 meV to 80 ± 5 meV. While the magnitude of this correction is subject to several uncertainties, this exercise does provide an appreciation for the size of this effect in these systems, implying that it is minor.

The ion–solvent dissociation energy of $NO^-(Ar)_1$ is given by rearranging Eq. (3)

$$D_o[NO^-\cdots Ar] = EA[NO(Ar)] - EA[NO] + D_{WB}[NO\cdots Ar]. \quad (9)$$

Using 84 meV as our experimentally determined value of EA[NO(Ar)], 26 meV as the literature value for EA[NO], and 10 meV as the literature value for $D_{WB}[NO\cdots Ar]$, gives 68 meV for $D_o[NO^-\cdots Ar]$, as already mentioned. Then, employing the -4 meV correction to EA[NO(Ar)] from above yields 64 meV for $D_o[NO^-\cdots Ar]$. Interestingly, Chalasinski's[95] calculations predict D_e for $NO^-(Ar)$ to be 509 cm^{-1} (63 meV). This discussion might seem to suggest a need to further refine the D_o values used to make Fig. 9. However, since we do not know the analogous corrections to the EAs of $NO(Kr)_1$ and $NO(Xe)_1$, and since, in any case, they would have a near-negligible effect on extrapolated D_o values derived from this plot, we have not attempted to improve the D_o's used to make it.

We close this section with a word about the practicality of the approximation in Eq. (6), and we illustrate the point for anion–rare-gas systems with $NO^-(Ar)_1$ and Eq. (9). While the neglect of $D_{WB}[NO\cdots Ar]$, called for in the approximation, causes $D_o[NO^-\cdots Ar]$ to be underestimated, the use of $SE_{step}(1)$, i.e., EA[NO(Ar)]–EA[NO], has the opposite effect, since uncorrected EA[NO(Ar)] values tend to be slightly too large. Thus, in the practical application of this commonly used approximation, there is a partial compensation of unknowns that leads to somewhat better values for ion–solvent dissociation energies than one might have expected, *viz.*, $D_0[NO^-\cdots Ar]=58$ meV using the approximation versus 64 meV upon applying both corrections.

C. $NO^-(H_2S)_1$, $NO^-(NH_3)_1$, $NO^-(H_2O)_1$, and $NO^-(EG)_1$

The photoelectron spectrum of $NO^-(H_2S)_1$ shows the characteristic spectral fingerprint of the NO^- subion, and is presented in Fig. 5. The photoelectron spectrum of $NO^-(EG)_1$ is shown in Fig. 6(a), and neither it nor the photoelectron spectrum of $NO^-(NH_3)_1$ shows a resolved NO^- subion profile. Note, however, that the NO^- subion profile fits neatly within the $NO^-(EG)_1$ spectrum [see Fig. 6(b)], permitting the extraction of the (0,0) transition energy for $NO^-(EG)_1$. The (0,0) transition energy for $NO^-(NH_3)_1$ was extracted from its photoelectron spectrum in an analogous way. The same kind of behavior was seen for $NO^-(H_2O)_1$ in our previous study of it.[68] There too, the spectral profile of the NO^- subion fit nicely within the unresolved photoelectron spectrum of $NO^-(H_2O)_1$, indicating that its features had been broadened by its interaction with water. We presume that the same has happened in the cases of $NO^-(EG)_1$ and $NO^-(NH_3)_1$. The $SE_{step}(1)$ values (recall that $SE_{step}\approx D_0$) for all four of these anion–molecule complexes are listed in Table V, where their ion–neutral interaction energies are seen to decrease in the order: $NO^-(EG)_1$, $NO^-(H_2O)_1$, $NO^-(NH_3)_1$, $NO^-(H_2S)_1$. It appears that the extent of spectral broadening in their photoelectron spectra is related to the strength of their ion–neutral interactions. Also, notice that NH_3 behaves more like H_2O than does H_2S, probably reflecting the relatively weak hydrogen bonding propensity of H_2S.

VII. SUMMARY OF SE_{tot} VERSUS n RESULTS FOR THE SYSTEMS STUDIED

The present photoelectron study of $NO^-(Y)_n$ cluster ions complements the two other photoelectron studies on solvated nitric oxide anion systems that we have conducted previously.[64,68] The energetics for all of the $NO^-(Y)_n$ species we have studied to date are summarized in Fig. 10 [see Fig. 7 for $n=7-14$ in $NO^-(Ar)_n$]. Figure 10 plots $SE_{tot}(n)$ versus n for $NO^-(EG)_{1,2}$, $NO^-(H_2O)_{1,2}$, $NO^-(NH_3)_1$, $NO^-(H_2S)_1$, $NO^-(N_2O)_{1-5}$, $NO^-(Xe)_{1-4}$, $NO^-(Kr)_1$, and $NO^-(Ar)_{1-6}$. Taken together, the data plotted here reflect the considerable range of interactions involved in ion–neutral bonding.

ACKNOWLEDGMENTS

We thank Bill Klemperer for several enjoyable conversations regarding this work, George Pisiello for expert fabrication of the ion source components, and Scott Witonsky for his help in preparing some of the figures. We gratefully acknowledge support for this work from the National Science Foundation. Acknowledgment is also made to the Donors of The Petroleum Research Fund, administered by the American Chemical Society, for partial support of this research. We also thank Mario Fajardo for sharing his results on the structure of $O^-(Ar)_2$ prior to publication.

[1] A. W. Castleman, Jr. and K. H. Bowen, Jr., J. Phys. Chem. **100**, 12911 (1996).
[2] G. H. F. Diercksen and W. P. Kraemer, Chem. Phys. Lett. **5**, 570 (1970).
[3] W. P. Kraemer and G. H. F. Diercksen, Theor. Chim. Acta **27**, 365 (1972).
[4] H. Kistenmacher, H. Popkie, and E. Clementi, J. Chem. Phys. **58**, 5627 (1973).
[5] H. Kistenmacher, H. Popkie, and E. Clementi, J. Chem. Phys. **61**, 799 (1974).
[6] P. Schuster, W. Jakubetz, and W. Marius, *Molecular Models for the Solvation of Small Ions and Polar Molecules* (Springer, Berlin, 1975).
[7] B. O. Roos, W. P. Kraemer, and G. H. F. Diercksen, Theor. Chim. Acta **42**, 77 (1976).
[8] K. G. Spears and S. N. Kim, J. Phys. Chem. **80**, 673 (1976).
[9] F. F. Abraham, M. R. Mruzik, and G. N. Pound, Faraday Discuss. Chem. Soc. **61**, 34 (1976).
[10] P. A. Kollman, Acc. Chem. Res. **10**, 365 (1977).
[11] C. Tsoo, D. A. Estrin, and S. J. Singer, J. Chem. Phys. **93**, 7187 (1990).
[12] L. Perera and M. Berkowitz, J. Chem. Phys. **95**, 1954 (1991).
[13] L. Perera and M. Berkowitz, J. Chem. Phys. **96**, 8288 (1992).
[14] L. Perera and M. Berkowitz, J. Chem. Phys. **99**, 4222 (1993).
[15] L. Perera and M. Berkowitz, J. Chem. Phys. **100**, 3085 (1994).
[16] I. Rips and J. Jortner, J. Chem. Phys. **97**, 536 (1992).
[17] J. E. Combariza, N. R. Kestner, and J. Jortner, J. Chem. Phys. **100**, 2851 (1994).
[18] R. L. Asher, D. A. Micha, and P. J. Brucat, J. Chem. Phys. **96**, 7683 (1992).
[19] T. Asado, K. Nishimoto, and K. Kitaura, J. Phys. Chem. **97**, 7724 (1993).
[20] N. Lee, R. G. Keesee, and A. W. Castleman, Jr., J. Chem. Phys. **72**, 1089 (1980).

[21] R. G. Keesee, N. Lee, and A. W. Castleman, Jr., J. Am. Chem. Soc. **101**, 2599 (1979).
[22] R. G. Keesee, N. Lee, A. W. Castleman, Jr., J. Geophys. Res. **84**, 3719 (1979).
[23] P. Kebarle, M. Arshadi, and J. Scarborough, J. Chem. Phys. **49**, 817 (1968).
[24] M. Arshadi and P. Kebarle, J. Phys. Chem. **74**, 1483 (1970).
[25] J. D. Payzant, R. Yamdagni, and P. Kebarle, Can. J. Chem. **49**, 3308 (1971).
[26] P. Yamdagni and P. Kebarle, J. Am. Chem. Soc. **93**, 7139 (1971).
[27] R. Yamdagni and P. Kebarle, Can. J. Chem. **52**, 2449 (1974).
[28] J. A. Davidson, F. C. Fehsenfeld, and C. Howard, Int. J. Chem. Kinet. **9**, 17 (1977).
[29] J. M. Riveros, Adv. Mass Spectrom. **33**, 362 (1975).
[30] M. Depaz, A. G. Giardini, and L. Friedman, J. Chem. Phys. **52**, 687 (1970).
[31] E. E. Ferguson, F. C. Fehsenfeld, and D. L. Albritton, in *Gas Phase Ion Chemistry*, edited by M. T. Bowers (Academic, New York, 1979), Vol. 1, pp. 45–82.
[32] A. Good, Chem. Rev. **75**, 561 (1975).
[33] E. E. Ferguson, in *Kinetics of Ion-Molecule Reactions*, edited by P. Ausloos (Plenum, New York, 1978).
[34] F. C. Fehsenfeld, P. J. Crutzen, A. L. Schmeltekopf, C. J. Howard, D. L. Albritton, E. E. Ferguson, J. A. Davidson, and H. I. Schiff, J. Geophys. Res. **81**, 4454 (1976).
[35] C. L. Howard, F. C. Fehsenfeld, and M. McFarland, J. Chem. Phys. **60**, 5086 (1974).
[36] E. W. McDaniel and N. R. C. McDowell, Phys. Rev. **114**, 1028 (1959).
[37] H. W. Ellis, R. Y. Pai, I. R. Gatland, E. W. McDaniel, R. Wernlund, and M. J. Cohen, J. Chem. Phys. **64**, 3935 (1976).
[38] H. S. Carman, Jr., J. Chem. Phys. **100**, 2629 (1994).
[39] K. H. Bowen, G. W. Liesegang, R. A. Sanders, and D. R. Herschbach, J. Phys. Chem. **87**, 557 (1983).
[40] J. A. Burt, Geophys. Res. **77**, 6289 (1972).
[41] P. C. Cosby, R. A. Bennett, J. R. Peterson, and J. T. Moseley, J. Chem. Phys. **63**, 1612 (1975).
[42] P. C. Cosby, J. H. Ling, J. R. Peterson, and J. T. Moseley, J. Chem. Phys. **65**, 5267 (1976).
[43] M. L. Vestal and G. H. Mauclaire, J. Chem. Phys. **67**, 3758 (1977).
[44] P. C. Cosby, G. P. Smith, and J. T. Moseley, J. Chem. Phys. **69**, 2779 (1978).
[45] G. P. Smith and L. C. Lee, J. Chem. Phys. **71**, 2323 (1979).
[46] R. V. Hodges, L. C. Lee, and J. T. Moseley, J. Chem. Phys. **72**, 2998 (1980).
[47] A. W. Castleman, Jr., P. M. Holland, D. E. Hunton, R. G. Keesee, T. G. Lindeman, K. I. Peterson, F. J. Schelling, and B. D. Upschulte, Ber. Bunsenges. Phys. Chem. **86**, 866 (1982).
[48] J. A. Burt, J. Chem. Phys. **57**, 4649 (1972).
[49] A. W. Castleman, Jr., D. E. Hunton, T. G. Lindeman, and D. N. Lindsay, Int. J. Mass Spectrom. Ion Phys. **47**, 199 (1983).
[50] J. F. Winkel, A. B. Jones, C. A. Woodward, D. A. Kirkwood, and A. J. Stace, J. Chem. Phys. **101**, 9436 (1994).
[51] J. A. Draves, Z. Luthey-Schulten, W. L. Lilu, and J. M. Lisy, J. Chem. Phys. **93**, 4589 (1990).
[52] M. Okamura, L. I. Yeh, and Y. T. Lee, J. Chem. Phys. **88**, 79 (1988).
[53] J. M. Price, M. W. Crofton, and Y. T. Lee, J. Chem. Phys. **91**, 2749 (1989).
[54] L. F. Dimauro, M. Heaven, and T. A. Miller, Chem. Phys. Lett. **104**, 526 (1984).
[55] H.-S. Kim and M. T. Bowers, J. Chem. Phys. **85**, 2718 (1986).
[56] L. A. Posey, M. J. DeLuca, and M. A. Johnson, Chem. Phys. Lett. **131**, 170 (1986).
[57] M. L. Alexander, M. A. Johnson, N. E. Levinger, and W. C. Lineberger, Phys. Rev. Lett. **57**, 976 (1986).
[58] C. C. Arnold, D. M. Neumark, D. M. Cyr, and M. A. Johnson, J. Phys. Chem. **99**, 1633 (1995).
[59] M. F. Jarrold, A. J. Illies, and M. T. Bowers, J. Chem. Phys. **82**, 1832 (1985).
[60] B. Pozinak and R. C. Dunbar, Int. J. Mass Spectrom. Ion Processes **133**, 97 (1994).
[61] J. M. Papanikolas, J. R. Gord, N. E. Levinger, D. R. Ray, V. Vorsa, and W. C. Lineberger, J. Phys. Chem. **95**, 8028 (1991).
[62] S. Golub and B. Steiner, J. Chem. Phys. **49**, 5191 (1968).
[63] J. V. Coe, J. T. Snodgrass, C. B. Freidhoff, K. M. McHugh, and K. H. Bowen, J. Chem. Phys. **83**, 3169 (1985).
[64] J. V. Coe, J. T. Snodgrass, C. B. Freidhoff, K. M. McHugh, and K. H. Bowen, J. Chem. Phys. **87**, 4302 (1987).
[65] K. H. Bowen and J. G. Eaton, in *The Structure of Small Molecules and Ions*, edited by R. Naaman and Z. Vager (Plenum, New York, 1988).
[66] J. V. Coe, J. T. Snodgrass, C. B. Freidhoff, K. M. McHugh, and K. H. Bowen, J. Chem. Phys. **83**, 3169 (1985).
[67] J. T. Snodgrass, J. V. Coe, C. B. Freidhoff, K. M. McHugh, and K. H. Bowen, Faraday Discuss. Chem. Soc. **86**, 241 (1988).
[68] J. G. Eaton, S. T. Arnold, and K. H. Bowen, Int. J. Mass Spectrom. Ion Processes **102**, 303 (1990).
[69] S. T. Arnold, J. H. Hendricks, and K. H. Bowen, J. Chem. Phys. **102**, 39 (1995).
[70] J. V. Coe, J. T. Snodgrass, C. B. Freidhoff, K. M. McHugh, and K. H. Bowen, Chem. Phys. Lett. **124**, 274 (1986).
[71] J. T. Snodgrass, J. V. Coe, C. B. Freidhoff, K. M. McHugh, and K. H. Bowen, J. Chem. Phys. **88**, 8014 (1988).
[72] J. T. Snodgrass, J. V. Coe, C. B. Freidhoff, K. M. McHugh, and K. H. Bowen, J. Phys. Chem. **99**, 9675 (1995).
[73] T. M. Miller, D. G. Leopold, K. K. Murray, and W. C. Lineberger, Bull. Am. Phys. Soc. **30**, 880 (1985).
[74] L. A. Posey, M. J. Deluca, and M. A. Johnson, Chem. Phys. Lett. **131**, 170 (1986).
[75] D. M. Cyr, G. A. Bishea, M. G. Scarton, and M. A. Johnsom, J. Chem. Phys. **97**, 5911 (1992).
[76] L. A. Posey and M. A. Johnson, J. Chem. Phys. **88**, 5383 (1988).
[77] M. J. DeLuca, B. Liu, and M. A. Johnson, J. Chem. Phys. **88**, 5857 (1988).
[78] C. E. H. Dessent, C. G. Bailey, and M. A. Johnson, J. Chem. Phys. **103**, 2006 (1995).
[79] G. Markovich, S. Pollack, R. Giniger, and O. Cheshnovsky, J. Chem. Phys. **101**, 9344 (1994).
[80] G. Markovitch, R. Giniger, M. Levin, and O. Cheshnovsky, Z. Phys. D: At., Mol. Clusters **20**, 69 (1991).
[81] G. Markovich, O. Cheshnovsky, and U. Kaldor, J. Chem. Phys. **99**, 6201 (1993).
[82] D. W. Arnold, S. E. Bradforth, E. H. Kim, and D. M. Neumark, J. Chem. Phys. **102**, 3510 (1995).
[83] D. W. Arnold, S. E. Bradforth, E. H. Kim, and D. M. Neumark, J. Chem. Phys. **97**, 9468 (1992).
[84] D. W. Arnold, S. E. Bradforth, E. H. Kim, and D. M. Neumark, J. Chem. Phys. **102**, 3493 (1995).
[85] T. Nagata, H. Yoshida, and T. Kondow, Chem. Phys. Lett. **199**, 205 (1992).
[86] C. R. Moylan, J. A. Dodd, C. C. Han, and J. I. Brauman, J. Chem. Phys. **86**, 5350 (1987).
[87] C. R. Moylan, J. A. Dodd, and J. I. Brauman, Chem. Phys. Lett. **118**, 38 (1985).
[88] D. M. Wetzel and J. I. Brauman, Chem. Rev. **87**, 607 (1987).
[89] J. V. Coe, J. T. Snodgrass, C. B. Freidhoff, K. M. McHugh, and K. H. Bowen, J. Chem. Phys. **84**, 618 (1986).
[90] M. J. Travers, D. C. Cowles, and G. B. Ellison, Chem. Phys. Lett. **164**, 450 (1989).
[91] M. W. Siegel, R. J. Celotta, J. L. Hall, J. Levine, and R. A. Bennett, Phys. Rev. A **6**, 607 (1972).
[92] K. P. Huber and G. Herzberg, in *Molecular Spectra and Molecular Structure*, Vol. IV, Constants of Diatomic Molecules (Van Nostrand Reinhold, New York, 1979).
[93] D. Teillet-Billy and F. Fiquet-Fayard, J. Phys. B **10**, L111 (1977).
[94] S. R. Desai, C. S. Feigerle, and J. C. Miller, J. Chem. Phys. **97**, 1793 (1992).
[95] G. Chalasinski and B. Kukawska-Tarnawska, J. Phys. Chem. **94**, 3450 (1990).
[96] E. A. Colbourn and A. E. Douglas, J. Chem. Phys. **65**, 1741 (1976).
[97] P. R. Herman, P. E. La Rocque, and B. P. Stoicheff, J. Chem. Phys. **89**, 4535 (1988).
[98] F. G. Amar, in *Physics and Chemistry of Small Clusters*, edited by P. Jena, B. K. Rao, and S. N. Khanna (Plenum, New York, 1987), p. 207.
[99] J. H. Hendricks, H. L. de Clercq, S. T. Arnold, and K. H. Bowen (unpublished).
[100] M. Fajardo (private communication, 1998).
[101] K. Hiraoka, S. Fujimaki, K. Aruga, and S. Yamabe, J. Phys. Chem. **98**,

8295 (1994); K. Hiraoka, S. Fujimaki, K. Aruga, T. Sato, and S. Yamabe, J. Chem. Phys. **101**, 4073 (1994).
[102] J. C. Miller, J. Phys. Chem. **90**, 4031 (1989).
[103] K. Sato, Y. Achiba, and K. Kimura, J. Chem. Phys. **81**, 57 (1984).
[104] H. H. W. Thuis, S. Stolte, J. Reuss, J. J. H. van den Biesen, and C. J. N. van den Meijdenberg, Chem. Phys. **52**, 211 (1980).
[105] P. Casavecchia, A. Laganà, and G. G. Volpi, Chem. Phys. Lett. **112**, 445 (1984).
[106] J. Nieman and R. Naaman, J. Chem. Phys. **84**, 3825 (1986).
[107] M. H. Alexander, J. Chem. Phys. **99**, 7725 (1993).
[108] *CRC Handbook of Chemistry and Physics*, 71st ed., edited by D. R. Lide (CRC, Ann Arbor, MI, 1991).
[109] A. A. Radziq and B. M. Smirnov, *Reference Data on Atoms, Molecules, and Ions* (Springer, Berlin Heidelberg, 1985).
[110] Taken from Adv. At. Mol. Phys. **13**, 210 (1977).